# Numerical Investigation of Strain Distribution During Cyclic Expansion Extrusion (CEE)

**H. Torabi[a], M. M. Samandari[a], G. Faraji[a,*], A. Masoumi[a]**

[a,] *Department of Mechanical Engineering, University College of Engineering, University of Tehran, Tehran, Iran.*

**ARTICLE INFO**

*Article history:*

Received 07 February 2015
Accepted 09 June 2015
Available online 30 June 2015

*Keywords:*

Cyclic Expansion Extrusions (CEE)
strain distribution
Deformation Zone (DZ)
Homogeneity

**ABSTRACT**

Strain distribution of Al 1100 was numerically investigated during cyclic expansion extrusion (CEE) process using finite element method (FEM). Die angle, corner fillet radius and die chamber diameter were considered as die parameters and friction factor and number of passes as process parameters. The effects of these parameters were investigated on the effective strain and strain homogeneity in the CEE process. Results showed that the decrease of friction factor along with the increase of die angle, corner fillet radius and number of passes lead to more homogeneous strain distribution, while chamber diameter has an optimal effect on the homogeneity. Material flow diagram of the deformation zone demonstrated that shear strains have a significant contribution to accumulated effective strain especially adjacent to the outer region of the sample. In comparison, in the central region of the CEE processed sample, normal strains exist as a dominant deformation route. Also, the results revealed that all the parameters except corner fillet radius (r) influence on the equivalent strain value.

## 1. Introduction

Processes with severe plastic deformation (SPD) may be defined as metal forming processes in which an ultra-large plastic strain is applied to create ultra-fine grained (UFG) and nanostructured metals[1-4].Many investigations over the last decade have been devoted to the applications of SPD in processing materials due to the superior and unique mechanical and physical properties of these structures fabricated by SPD techniques[5, 6].In this regard, various SPD techniques such as equal channel angular pressing (ECAP)[5, 7], accumulative rollbonding (ARB)[8, 9], high pressure torsion (HPT)[10, 11], cyclic extrusion compression (CEC)[12, 13], and many other processes have beendeveloped[5, 14, 15].Cyclic expansion extrusion (CEE) process was proposed by Pardis et al. [16]as a modified counterpart of cyclic extrusion-compression (CEC)and based on this process, a new SPD method was proposed by Babaei et al. for production of UFG tubes, entitled as TCEE[17]. Also, an investigationintroduces two new processing routes for CEE of rectangular cross sections [18]. In this newly proposed process, the extrusion part of the process is carried out after the material experiences expansion. Although there are some reported researches for

Corresponding author:
*E-mail address:* ghfaraji@ut.ac.ir (G. Faraji).

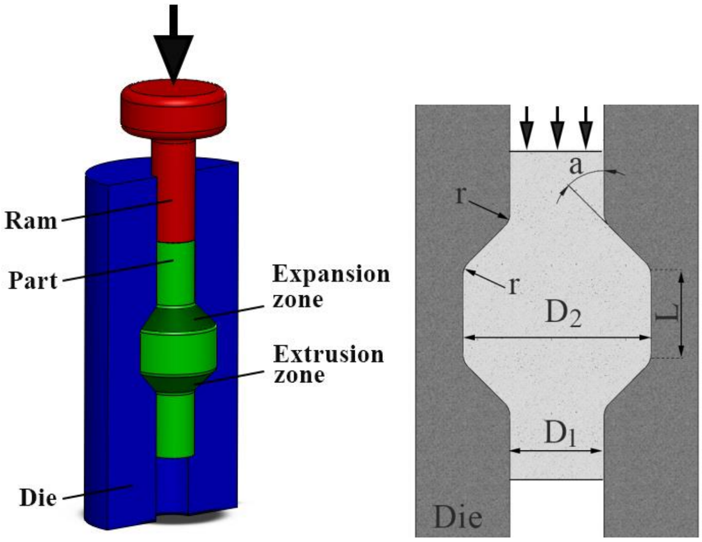


**Fig. 1.** Schematic illustrations of CEE process and die design parameters

investigation of strain distribution in CEC [19, 20]. Also, some researchers work on mechanical aspects of the process and analyze them by means of the finite element method (FEM) [21].This technique is a new method that has not been studiedin detail. In this article,FEM simulations are used to investigate the effects of the mentioned parameters on strain distribution in CEE process of circular cross sections.Schematic illustrations of the CEE process and die parameters areshown in Fig. 1. The CEE method is a cyclic process in which the crosssection of the material is increasedto the chamber diameter ($D_2$) and subsequently is extruded to initial diameter ($D_1$) while the material is passingthe deformation zone (DZ).Thus, the material undertakes two half cycles including expansionand extrusion. When the material passes through the DZ, the total accumulated strain can be calculated theoretically by Eq. (1)[16]. The first logarithm represents the strain in the expansion half-cycle and the second in the extrusion half-cycle.

$$\bar{\varepsilon}=Ln\left(\frac{D_2^2}{D_1^2}\right)-Ln\left(\frac{D_1^2}{D_2^2}\right) \quad [1]$$

The materials undertake both expansion and extrusion in each passand after*n* passes the accumulated strainin DZ can be measured by Eq. (2):

$$\bar{\varepsilon}=4\,n\,Ln\left(\frac{D_2}{D_1}\right) \quad [2]$$

One of the advantages of the CEE process in comparison withCEC is that the force needed to extrude the material is supposed to provide a proper amount of back-pressure for the expansion. Therefore, no external back-pressure system is required.

## 2. FEMProcedure

Simulations were done usingthecommercial DEFORM-3D software. An automatic remeshing was employed in the simulations to accommodate the imposed large strains tofurtherthe accuracy of the results. It is necessary to properly define the material behavior, boundary conditions and FEM parameters like elements and solving method. 1/16 of the work-piece and dies wassimulated in the FEM because of the symmetric nature of the process.Die angle ($a$), corner fillet radius ($r$), and die chamber diameter ($D_2$) were considered as die parametersas shown in Fig. 1. Also, friction factor($m$), and number of passeswere considered as process parameters for the investigation ofthe equivalent strain.The parameters and their values used in the simulationsarelisted in Table 1.The initial diameter of thecylindrical sampleand the length of the chamber ($L$) areequal to 10mm.FE parameters used for simulations aregivenin Table 2. Theengineering stress-straincurve of Al 1100 is shown in Fig. 2 [22].

**Table 1.**Variable parameters and simulation condition

| Variable parameter | Levels | Other parameters | | | | |
|---|---|---|---|---|---|---|
| | | *a* (º) | *r* (mm) | $D_2$ (mm) | *m* | *n* |
| Die angle (a) | 30, 45, 60, 75, 90 | - | 1 | 20 | 0.1 | 3 |
| corner fillet radius (r) | 0.5, 1, 1.5, 2 | 45 | - | 20 | 0.1 | 3 |
| die chamber diameter ($D_2$) | 15, 20, 25 | 45 | 1 | - | 0.1 | 3 |
| friction factor (m) | 0, 0.3, 0.6, 0.9 | 45 | 1 | 20 | - | 3 |
| number of passes (n) | 2, 4, 8, 16 | 45 | 1 | 20 | 0.1 | - |

**Table 2.** FE parameters used for simulations

| Parameter | Value | |
|---|---|---|
| | Die | Workpiece |
| Material | Rigid | Al 1100 |
| Temperature (ºC) | 20 | 20 |
| Density (g/cm$^3$) | - | 2.71 |
| Young's modulus (GPa) | - | 70 |
| Poisson's ratio | - | 0.33 |
| Type of elements | Tetrahedral | |

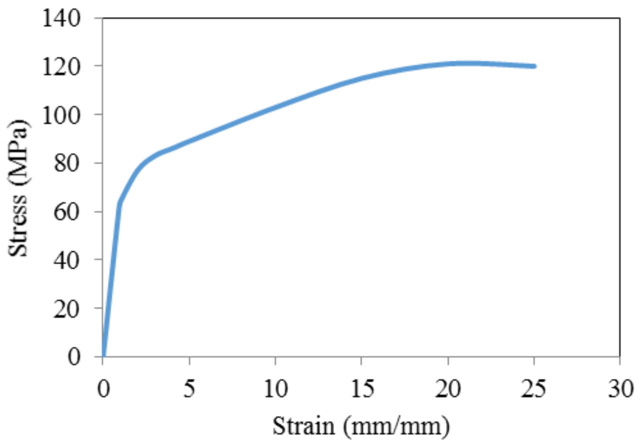


**Fig. 2.** Material behavior of Al 1100 at room temperature[22]**.**

## 3. Results and Discussion

### *3. 1. Strain Distribution in Deformation Zone*

Because of theaccumulation of redundant material in the chamber, both expansion and extrusion will not usually occur in each pass for all elements of the material. In addition, the material experiences shear strainsin the DZ. Fig. 3(a) shows the deformation velocity field (tothe left side) and deformation flow-net diagram (tothe right side).In Fig. 3(a)circle compression depicts normal strains(whichcan be calculated theoretically from Eq. 1) and circle rotation shows shear strains. Along the center line, normal strain contribution of effective strain is dominant and thus the theoretical equation is in good agreement with the FEM results (Fig. 3(b)).

### *3. 2. Strain history*

Fig.4 shows the strain history of five elements initially placed in the cross section of thecylindrical sample and move withthematerial flow in the CEE process. It can be seen that for each element, the strain increases gradually withanapproximately constant slope in 16 passes of the CEE process. It is obvious from this figure that by increasing the distance of the element from the center line the accumulated strainincreases. This is due tothe additional shear strains in these areas.

### *3. 3. Die parameters*

Fig. 5 shows the distribution of equivalent strain in the work-pieceafter 3 passes ofthe CEE process with different die angles. Other

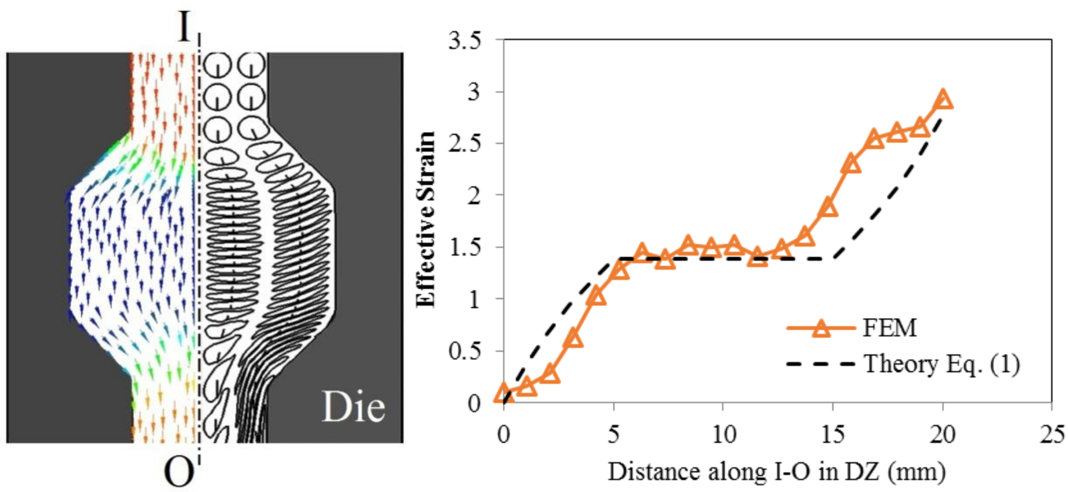


**Fig. 3.** Strain distributions in DZ (a) and effective strain along thecenter line (b); a=45°, r=1mm, $D_2$=20mm and m=0.1

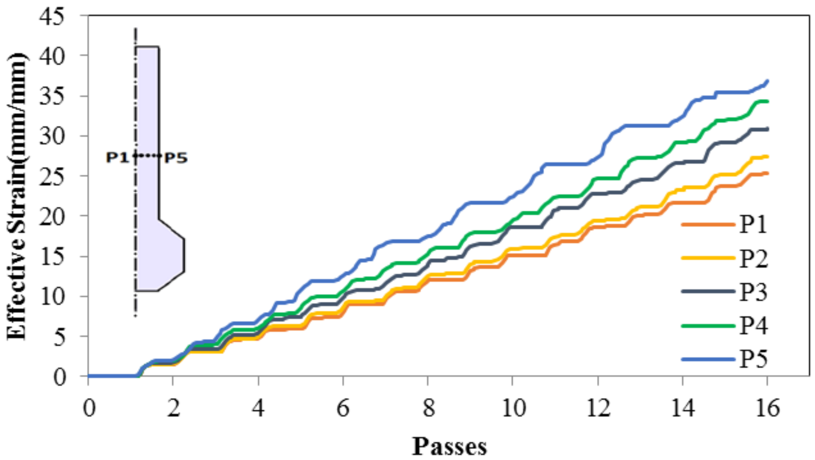


**Fig. 4.** Strain history of 5 elements in the cross section of thecylindrical sample, a=45°, r=1mm, $D_2$=20mm, and m=0.1

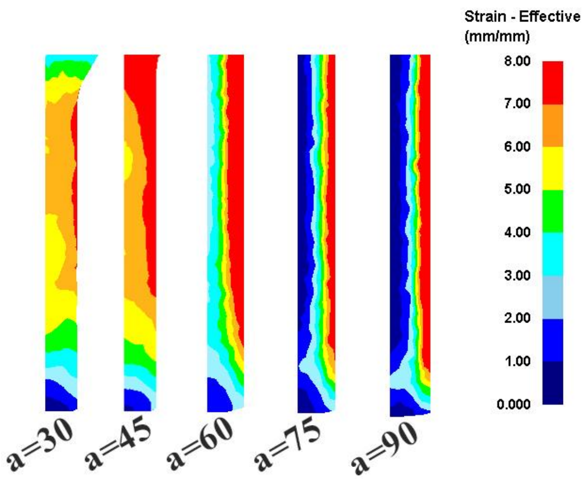


**Fig. 5.** Distribution of equivalent strain in the work-piece after 3passes ofthe CEE process with different die angles

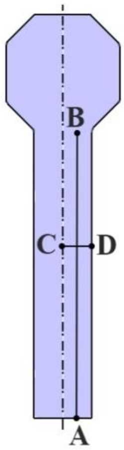


**Fig. 6.** Illustration of the paths for investigation of strain distribution in longitudinal (A-B) and lateral (C-D) directions

process parameters were considered as $D_2$=20 mm, r=1 mm, μ=0.1 and v=1 mm/s. As can be seen, the increase indie angles from 30° to 90° results in more inhomogeneity in the strain distribution.This result is in good agreement with the work done on ZK60 alloy in CEC by Lin et al.[19].

The lines A-B and C-D are defined (as illustrated in Fig. 6) to investigate the distribution of equivalent strain during and after the process. The distributions of equivalent strain along these lines are shown at different die angles in Fig. 7.This figure shows that thehomogeneity in the longitudinal direction does not vary widely with anincreasein thedie angle, whilethestrain distributions from center to thesurface vary in thebroad range. However, the change in strain distribution for 30˚, 45˚ and 75˚, 90˚ is not remarkable, and only a little increase in strain is observed. It is obvious that this inhomogeneity withanincrease of die angle is due to theinability of the work-piece to fluent material flow in DZ.

As discussed earlier, lower die angle has more uniform strain. Although the45˚ angle has more strain value in comparison with that of 30˚,both show almost similar strain homogeneity. As more strain is more desirable in severe plastic deformation processes, it can be concluded that within the 5 investigated angles above, angle of 45˚ is the most appropriate for more uniformity and strain value.

Corner radius has been investigated with variations from 0 to 2 mm with 0.5 mm steps. Fig. 8 shows the distribution of equivalent strain in the work-piece with increasing corner radius after 3-pass CEE. Other process parameters were considered as D=20 mm, θ=45˚, μ=0.1 and v=1 mm/s. The figure shows that strain homogeneity increases with increasing radius, although this increase is not thatsignificant.This result shows a good agreement with the work done on ZK60 alloy in CEC by Lin et al. [19].

Fig. 9 shows longitudinal and lateral strain distribution in the work-piece with different corner radiuses. It can be seen that longitudinal strain distribution does not have any variation. However, lateral distribution varies with a small slope and radius 0 has the most inhomogeneity because of less fluency in the material flow, and the strain of thesurface is more than the center in comparison withother radii. However, except radius 0, other radiido not haveasignificant difference witheach other and homogeneity is nearly identical.

As discussed above, homogeneity does not change widely with avariation of radius except r=0. The case of*r*= 0.5 mm has astrain homogeneity of 1, 1.5 and2 while the strain value is more than others. So, within the five investigated radiir=0.5 would be the most appropriate value for more uniformity and strain value.

The diameter of thechamber is the other factor investigated for strain distribution withthe values of15, 20, 25mm. Other process

A

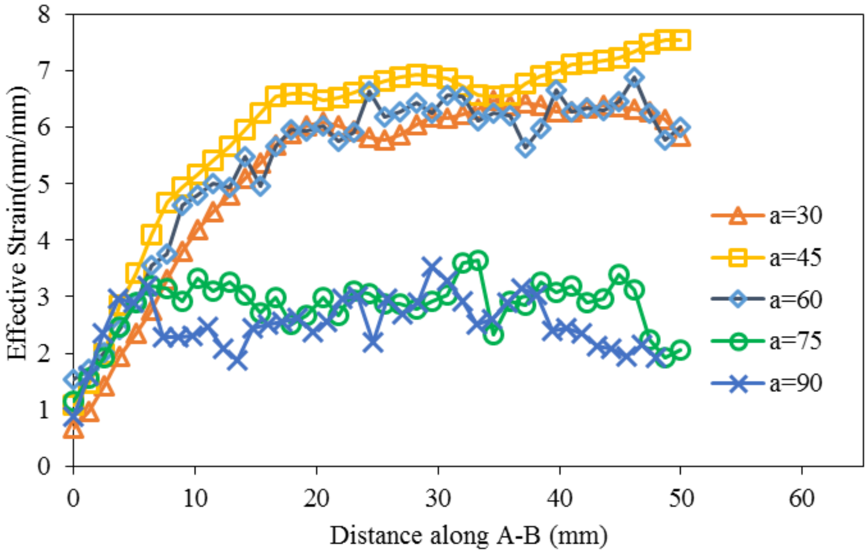


B

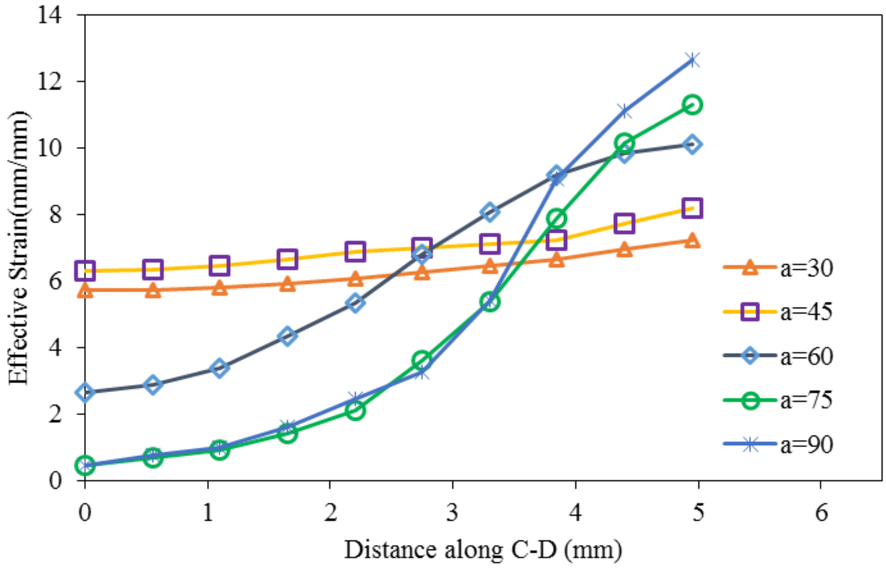


**Fig. 7.** Distribution of equivalent strain along the A-B and C-D lines inthework-piece at die angles of 30˚ to 90˚

parameters were considered as r=1 mm, a=45˚, m=0.1 and v=1 mm/s. Strain distribution is shown in Figs. 10 and 11. These figures show that the chamber diameter has a very smallimpact on strain homogeneity, and as can be seen in the Fig. 10, 11(a), the value of strain increases andbecause the slope of curves is almost equal, so the homogeneity for 3 cases is almost the same.However, inFig. 11(b), the slope of the curve for 15 mm has a jump inthe middle and variation of strain is more than other diameters. Also, the curve of thediameter of 25 mm has a bump while, in the diameter of 20 mm,it is almost smooth. Therfore, it can be concluded that the most appropriate longitudinal homogeneity is available for diameter of 20 mm.

As discussed before, chamber diameters do not change thelateral strain homogeneity, but for longitudinal strain distribution, 20 mm diameter gives more uniform strain compared tothe others. Also,thecomparison ofthe diameters of 20 and25 mmshows that thediameter of 25 mm produces more waste

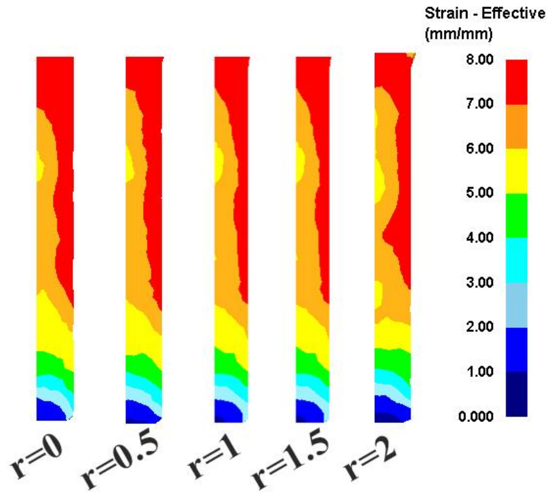


**Fig. 8.** Distribution of equivalent strain in the work-piece with increasing corner radius after three passes of CEE

A

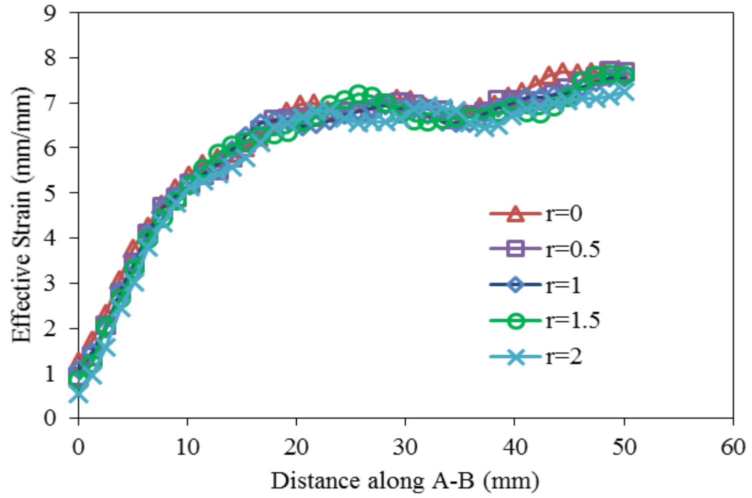


B

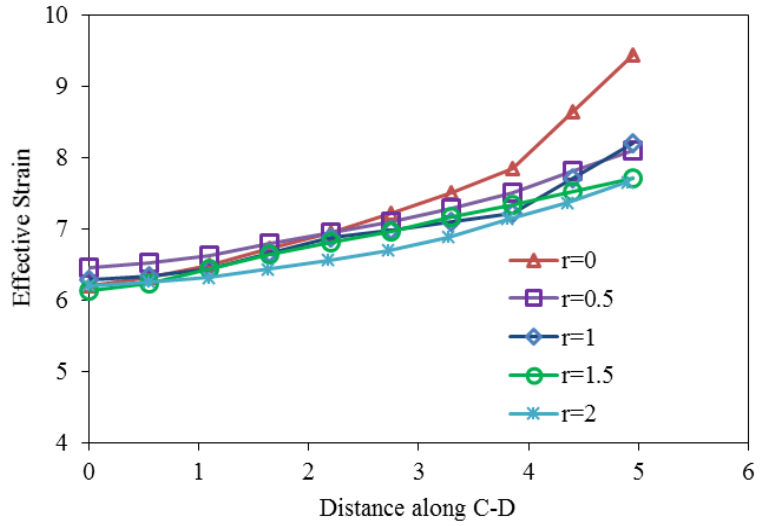


**Fig. 9.** Longitudinal and lateral strain distribution in the workpiece with corner radiuses of 0 to 2

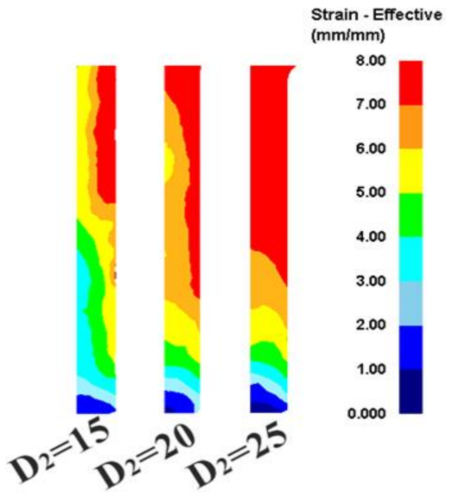


**Fig. 10.** Distribution of equivalent strain in the work-piece with increasing chamber diameter after threepasses CEE process

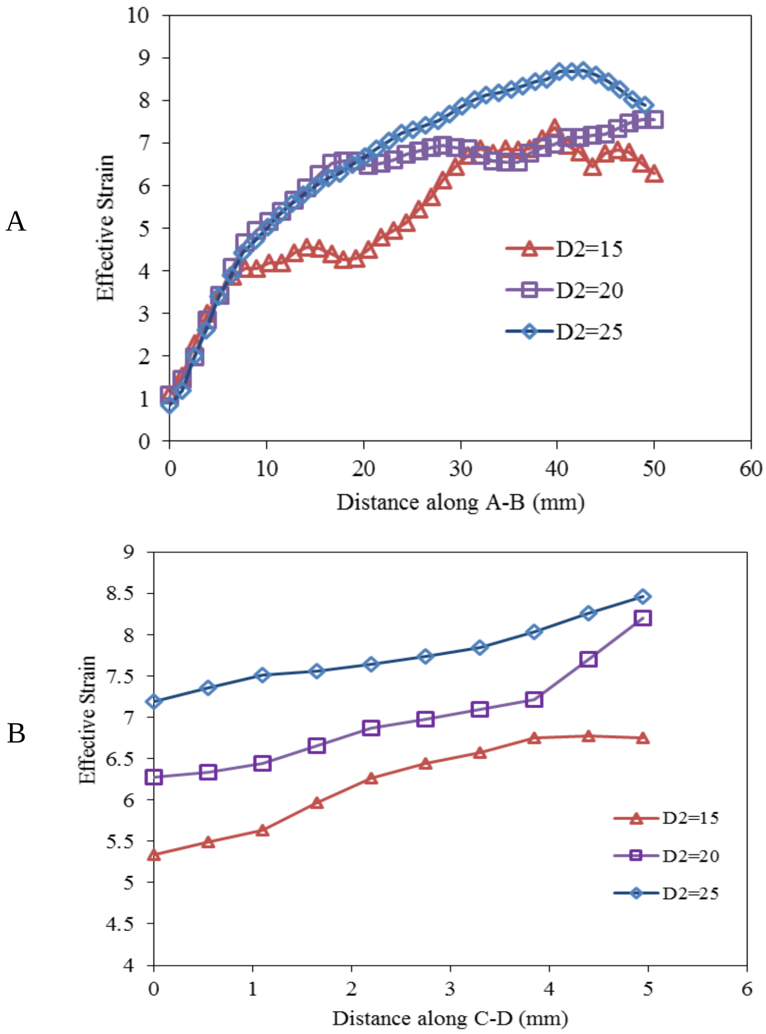


**Fig. 11.** Longitudinal and lateral strain distribution in the work-piece with chamber radiuses of 15, 20, 25 mm

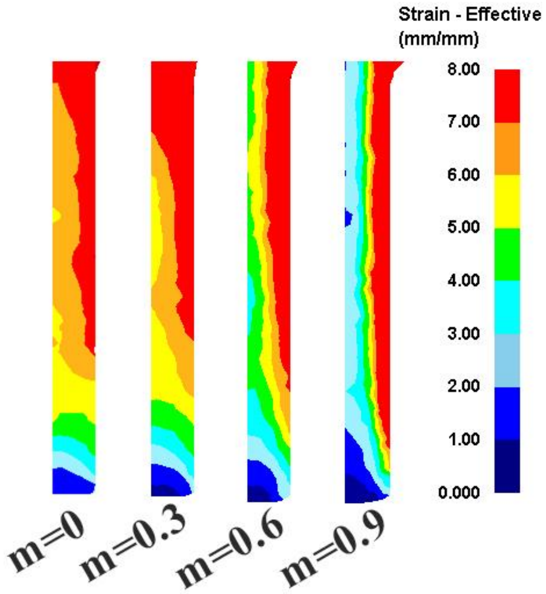


**Fig. 12.** Distribution of equivalent strain in the work-piece withavariation of the friction factor after 3-pass CEE

material compared to20 mm; thus,thediameter of 20 mm gives better results than the other investigated diameters.

### *3. 4. Process parameters*

The effect of friction factor has been investigated with values of m=0, 0.3, 0.6, 0.9. Other process parameters were considered as r=1 mm, a=45˚, $D_2$=20 mm and v=1 mm/s. Fig. 12 shows strain distribution in the final part after 3-pass CEE. As can be seen, strain distribution is so impressionable of friction and the strain of the center of the part is lower than the strain of the surface. This is also verified by the slope of the curves of Fig. 13(a). As the friction force on the surface increases, it results in the material flow at the surface to be more difficult than the center[23]. Therefore, the strain of the surface will become more than the center. It reveals that with decreasing of friction factor, the homogeneity of strain increases clearly.This result exhibits a good agreement with the work done on CEC of ZK60 alloy by Lin et al.[19].However, the longitudinal strain distribution is not more dependent onthe friction as it is shown in the Fig. 13(b). The slopes are almost equal, and it can be concluded that homogeneity will not vary in the length of the part withachange of the friction factor.

The effect of friction has been discussedabove, and it has been concluded that reduction of friction factor results in more uniform strain distribution. Though the friction is not practicallymore changeable, the lowest friction factors are more desirable to reach more homogeneous strain distribution.

Fig. 14 shows the effect of the number of passes on strain distribution. The number of passes was considered as 2, 4, 8, and 16. It is obvious that with an increase of passes, the value of strain will enhance because more strain-hardening is applied on the work-piece as shown in Fig. 14. As can be seen in this figure, strain homogeneity reduces withthe increase of pass numbers. In the pass numbers of 8 and 16, distribution of different colors is almost identical in the figures, but the maximum strain in the color bars increases withthe increase of the pass numbers.So, it shows that the variation of strain and inhomogeneity enhances withtheincrease of passes.

Fig. 15 shows longitudinal and lateral strain distribution in the work-piece in different number of passes. The increase of curves slopes in Fig. 15demonstrates that both longitudinal and lateral homogeneity decrease

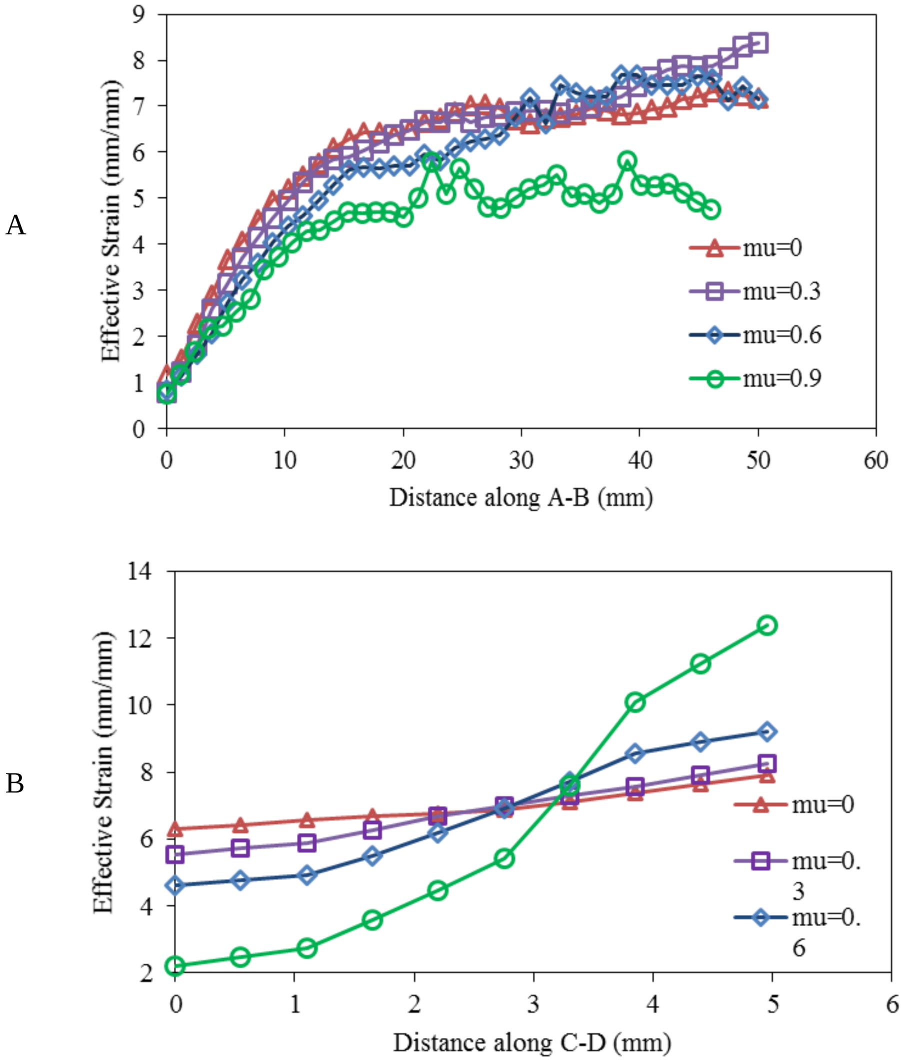


**Fig. 13.** Longitudinal and lateral strain distribution in the work-piece with the friction factors of 0, 0.3, 0.6 and 0.9

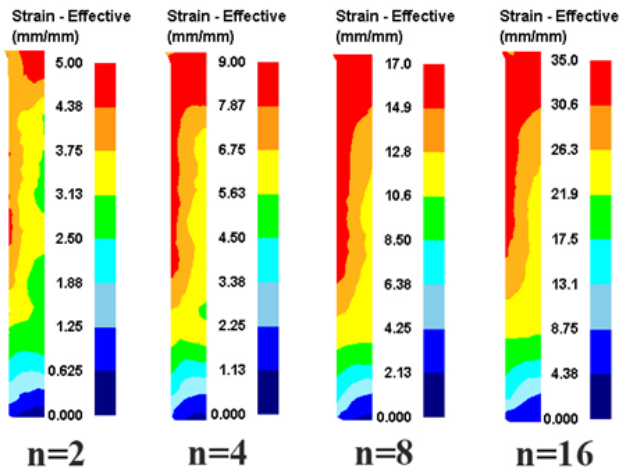


**Fig. 14.** Distribution of equivalent strain in the work-piece with increase the number of passes

A

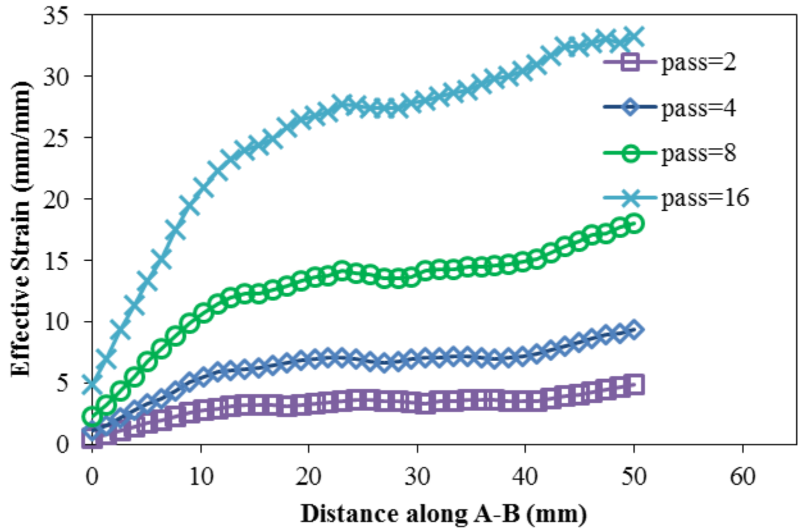


B

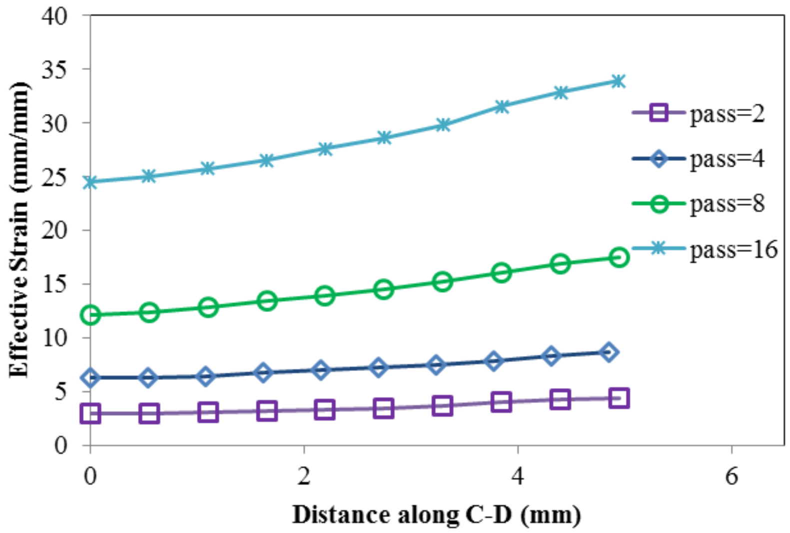


**Fig. 15.** Longitudinal and lateral strain distribution in the workpiece with passes of 2, 4, 8 and 16.

with increase the numbers of passes. Also, it is obvious in the figure that the values of strain enhance withtheincrease of passes. This result is in agreement with the work done on ZK60 alloy CEC in by Lin et al.[24].

As discussed above, increasing the number of passes causes increase of thestrain value and decrease of the strain homogeneity. Therefore, the most appropriate condition cannot be chosen, because two parameters are in conflict with each other. Therefore, according to the desired conditions (more strain value or more strain homogeneity) better conditions can be chosen.

## 4. Conclusions

The effects oftheprocess and die parameters on strain distribution were investigated during the CEE process of the Al 1100 samples. Results show that the die angle and friction factor have the most effect on lateral strain homogeneity.Therefore, the strain of the center of the part is much lower than surface strain withtheincrease of die angle and friction factor.Number of passes and die corner radius have lower effect on strain homogeneity in comparison withdie angle and friction factor; however, the center strain of the part is also lower than surface strain with increase of pass numbers and decrease of die corner radius. Chamber diameter hasaverysmalleffect on lateral strain distribution, but it has more effect on longitudinal homogeneity compared toother parameters so that homogeneity enhances withtheincrease of diameter. Other parameters have very low impact on longitudinal strain distribution. Material flow diagram of deformation zone showed that shear strains have significant contribution in accumulated effective strain especially adjacent to die surface.

## References


1. Horita, Z., Nanomaterials by Severe Plastic Deformation. International Conference on Nanomaterials by Severe Plastic Deformation 2006: Materials Science Forum. 1050.
2. Rosochowski, A., Processing metals by severe plastic deformation. Solid State Phenomena, 101, 2004, pp. 13-22.
3. Rosochowski, A., L. Olejnik, and M. Richert, Metal forming technology for producing bulk nanostructured metals. Journal of Steel and Related Materials–Steel GRIPS, 2, 2004, pp. 35-44.
4. Valiev, R., et al., Producing bulk ultrafine-grained materials by severe plastic deformation.JOM, 58(4), 2006, pp. 33-39.
5. Azushima, A., et al., Severe plastic deformation (SPD) processes for metals.CIRP Annals - Manufacturing Technology, 57(2), 2008, pp. 716-735.
6. Babaei, A. and M. M. Mashhadi, Characterization of ultrafine-grained aluminum tubes processed by Tube Cyclic Extrusion–Compression (TCEC). Materials Characterization, 95(0), 2014, pp. 118-128.
7. Valiev, R. Z. and T. G. Langdon, Principles of equal-channel angular pressing as a processing tool for grain refinement. Progress in Materials Science, 51(7), 2006, pp. 881-981.
8. Huang, X., et al., Microstructural evolution during accumulative roll-bonding of commercial purity aluminum. Materials Science and Engineering: A, 340(1–2), 2003, pp. 265-271.
9. Saito, Y., et al., Ultra-fine grained bulk aluminum produced by accumulative roll-bonding (ARB) process. Scripta Materialia, 39(9), 1998, pp. 1221-1227.
10. Zhilyaev, A. P., et al., Experimental parameters influencing grain refinement and microstructural evolution during high-pressure torsion. Acta Materialia, 51(3), 2003, pp. 753-765.
11. Zhilyaev, A. P. and T. G. Langdon, Using high-pressure torsion for metal processing: Fundamentals and applications. Progress in Materials Science, 53(6), 2008, pp. 893-979.
12. Richert, M., Q. Liu, and N. Hansen, Microstructural evolution over a large strain range in aluminium deformed by cyclic-extrusion–compression. Materials Science and Engineering: A, 260(1), 1999, pp. 275-283.
13. Zhang, J. A new bulk deformation method–Cyclic extrusion. in Materials Science Forum. 2007. Trans Tech Publ.
14. Faraji, G., et al., TEM analysis and determination of dislocation densities in nanostructured copper tube produced via parallel tubular channel angular pressing process. Materials Science and Engineering: A, 563(0), 2013, pp. 193-198.
15. Faraji, G. and M. Mousavi Mashhadia, Plastic deformation analysis in parallel tubular channel angular pressing (PTCAP). Journal of Advanced Materials and Processing, 1(4), 2013, pp. 23-32.
16. Pardis, N., et al., Cyclic expansion-extrusion (CEE): A modified counterpart of cyclic extrusion-compression (CEC). Materials Science and Engineering: A, 528(25–26), 2011, pp. 7537-7540.
17. Babaei, A., M. M. Mashhadi, and H. Jafarzadeh, Tube cyclic expansion-extrusion (TCEE) as a novel severe plastic deformation method for cylindrical tubes. Journal of Materials Science, 49(8), 2014, pp. 3158-3165.
18. Pardis, N., et al., Development of new routes of severe plastic deformation through cyclic expansion–extrusion process. Materials Science and Engineering: A, 613(0), 2014, pp. 357-364.

19. Lin, J.-b., et al., Finite element analysis of strain distribution in ZK60 Mg alloy during cyclic extrusion and compression. Transactions of Nonferrous Metals Society of China, 22(8), 2012, pp. 1902-1906.
20. Lin, J., et al., Study on deformation behavior and strain homogeneity during cyclic extrusion and compression. Journal of Materials Science, 43(21), 2008, pp. 6920-6924.
21. Rosochowski, A., R. Rodiet, and P. Lipinski, Finite element simulation of cyclic extrusion-compression. Metal Forming, 2000, pp. 253-259.
22. Azimi, A., et al., Mechanical properties and microstructural evolution during multi-pass ECAR of Al 1100–O alloy. Materials & Design, 42(0), 2012, pp. 388-394.
23. Faraji, G., et al., The role of friction in tubular channel angular pressing. Rev. Adv. Mater. Sci, 31, 2012, pp. 12-18.
24. Lin, J., et al., Study on deformation behavior and strain homogeneity during cyclic extrusion and compression. Journal of materials science, 43(21), 2008, pp. 6920-6924.